

Characterization of Cg10062 from *Corynebacterium glutamicum*: Implications for the Evolution of *cis*-3-Chloroacrylic Acid Dehalogenase Activity in the Tautomerase Superfamily[†]

Gerrit J. Poelarends,^{‡,§} Hector Serrano,^{§,||} Maria D. Person,[⊥] William H. Johnson, Jr.,^{||} and Christian P. Whitman^{*,||}

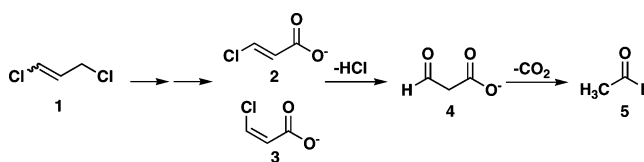
Department of Pharmaceutical Biology, Groningen Research Institute of Pharmacy, University of Groningen, Antonius Deusinglaan 1, 9713 AV Groningen, The Netherlands, and Divisions of Medicinal Chemistry and Pharmacology and Toxicology, College of Pharmacy, The University of Texas, Austin, Texas 78712-1074

Received April 25, 2008; Revised Manuscript Received June 2, 2008

ABSTRACT: A 149-amino acid protein designated Cg10062 is encoded by a gene from *Corynebacterium glutamicum*. The physiological function of Cg10062 is unknown, and the gene encoding this protein has no obvious genomic context. Sequence analysis links Cg10062 to the *cis*-3-chloroacrylic acid dehalogenase (*cis*-CaaD) family, one of the five known families of the tautomerase superfamily. The characterized tautomerase superfamily members have two distinctive characteristics: a β - α - β structure motif and a catalytic amino-terminal proline. Pro-1 is present in the Cg10062 amino acid sequence along with His-28, Arg-70, Arg-73, Tyr-103, and Glu-114, all of which have been implicated as critical residues for *cis*-CaaD activity. The gene for Cg10062 has been cloned and the protein overproduced, purified, and subjected to kinetic and mechanistic characterization. Like *cis*-CaaD, Cg10062 functions as a hydratase: it converts 2-oxo-3-pentynoate to acetopyruvate and processes 3-bromopropiolate to a species that inactivates the enzyme by acylation of Pro-1. Kinetic and ¹H NMR spectroscopic studies also show that Cg10062 processes both isomers of 3-chloroacrylic acid at low levels with a clear preference for the *cis* isomer. Pro-1 is critical for the dehalogenase and hydratase activities because the P1A mutant no longer catalyzes either reaction. The presence of the six key catalytic residues and the hydratase activity coupled with the absence of an efficient *cis*-CaaD activity and the lack of isomer specificity implicate factors beyond this core set of residues in *cis*-CaaD catalysis and specificity. This work sets the stage for in-depth mechanistic and structural studies of Cg10062, which could identify the additional features necessary for a fully active and highly specific *cis*-CaaD. Such results will also shed light on how *cis*-CaaD emerged in the tautomerase superfamily because Cg10062 could be characteristic of an intermediate along the evolutionary pathway for this dehalogenase.

The degradation of the nematocide 1,3-dichloropropene (**1**, Scheme 1) in *Pseudomonas pavonaceae* 170 is mediated by a series of enzymes with intriguing catalytic mechanisms and interesting evolutionary lineages (1–4). Three of these enzymes, *trans*-3-chloroacrylic acid dehalogenase (CaaD)¹ (5–8), *cis*-3-chloroacrylic acid dehalogenase (*cis*-CaaD) (9–11), and

Scheme 1



malonate semialdehyde decarboxylase (MSAD) (12, 13), represent three different families of the tautomerase superfamily, a group of structurally homologous proteins that share a characteristic β - α - β fold and a catalytic amino-terminal proline (14, 15).² CaaD and *cis*-CaaD convert the corresponding isomers of 3-chloroacrylate [2 and 3, respectively (Scheme 1)] to malonate semialdehyde (4). Subsequently, MSAD catalyzes the decarboxylation of 4 to yield acetaldehyde (5) and carbon dioxide (1–3).

Mechanistic and structural studies of CaaD, *cis*-CaaD, and MSAD have shown that the three enzymes are strikingly

[†] This research was supported by the National Institutes of Health Grant GM-65324. G.J.P. was supported by a VENI grant from the Division of Chemical Sciences of The Netherlands Organization of Scientific Research (NWO-CW).

* To whom correspondence should be addressed. Telephone: (512) 471-6198. Fax: (512) 232-2606. E-mail: whitman@mail.utexas.edu.

[‡] University of Groningen.

[§] These authors contributed equally to this work.

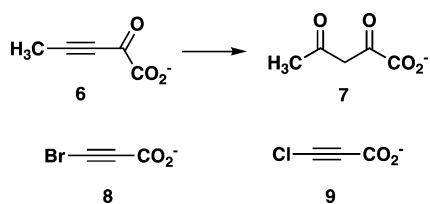
^{||} Division of Medicinal Chemistry, The University of Texas.

[⊥] Division of Pharmacology and Toxicology, The University of Texas.

¹ Abbreviations: Ap, ampicillin; CaaD, *trans*-3-chloroacrylic acid dehalogenase; *cis*-CaaD, *cis*-3-chloroacrylic acid dehalogenase; DMSO, dimethyl sulfoxide; ESI-MS, electrospray ionization mass spectrometry; HPLC, high-pressure liquid chromatography; LB, Luria-Bertani; MALDI-PSD, matrix-assisted laser desorption ionization postsource decay; MALDI-TOF, matrix-assisted laser desorption ionization time-of-flight; MSAD, malonate semialdehyde decarboxylase; NMR, nuclear magnetic resonance; 4-OT, 4-oxalocrotonate tautomerase; SDS–PAGE, sodium dodecyl sulfate–polyacrylamide gel electrophoresis.

² 5-(Carboxymethyl)-2-hydroxyruconate isomerase, a bacterial isomerase, and macrophage migration inhibitory factor, a cytokine with phenylpyruvate tautomerase activity, represent the other two families in the tautomerase superfamily (14, 15).

Scheme 2



similar, which likely reflects divergent evolution from an ancestral β - α - β template (11, 13). All three enzymes function as hydratases, converting 2-oxo-3-pentynoate (6, Scheme 2) to acetopyruvate (7), and require Pro-1 (with a pK_a of ~ 9.2) and two conserved arginines (α Arg-8 and α Arg-11 in CaaD, Arg-70 and Arg-73 in *cis*-CaaD, and Arg-73 and Arg-75 in MSAD) to catalyze this reaction as well as their physiological reactions (5–13). Moreover, as a result of this hydratase activity, the three enzymes convert the 3-halopropiolates (8 and 9, Scheme 2) to a reactive species (e.g., an acyl halide or a ketene) that results in the acylation of Pro-1 and enzyme inactivation (6, 9, 12). The three enzymes have a water-activating residue (α Glu-52 in CaaD, Glu-114 in *cis*-CaaD, and Asp-37 in MSAD), which has been implicated in the hydration reactions and the respective physiological activities (8, 11, 13). A common evolutionary history for the three enzymes is further strengthened by a comparison of the crystal structures, which show the core β - α - β unit, the common overall architecture, and the positional conservation of key catalytic residues (Pro-1 and the arginine pair) (11, 13).

In the course of a search for other *cis*-CaaD family members, a 149-amino acid protein from *Corynebacterium glutamicum*, designated Cg10062, was identified. The genomic context of the *cg10062* gene does not provide any clues about the biological function of this protein in *C. glutamicum*. The *cg10062* gene is flanked by genes encoding putative membrane proteins that might be involved in the transport of divalent metal ions and the diffusion of chloride ions. Although the sequence of Cg10062 is only 34% identical (and 53% similar) with that of *cis*-CaaD, six residues are present (Pro-1, His-28, Arg-70, Arg-73, Tyr-103, and Glu-114) that have been implicated as key players in the *cis*-CaaD mechanism (9, 11). Not surprisingly, it was found that Cg10062 catalyzes the hydration of 6 to 7 and the conversion of 8 to a species that covalently modifies Pro-1. Kinetic analysis of Cg10062 also shows that the enzyme has a low-level *cis*-CaaD activity and the ability to process the *trans* isomer (i.e., 2), in contrast to the highly specific *cis*-CaaD. The dehalogenase activity requires Pro-1, Arg-70, Arg-73, and Glu-114 as mutations at these positions render the enzyme inactive. The parallels between *cis*-CaaD and Cg10062 coupled with the absence of a robust *cis*-CaaD activity and isomer specificity in Cg10062 indicate that a fully functional *cis*-CaaD requires catalytic features and specificity determinants beyond the identified core set. As a result, Cg10062 could be representative of the type of intermediate template that gave rise to *cis*-CaaD.

MATERIALS AND METHODS

Materials. The sources of the chemicals, biochemicals, buffers, solvents, components of Luria-Bertani (LB) medium, and the enzymes and reagents used in the molecular biology

procedures are reported elsewhere (6, 9). Literature procedures were used for the synthesis of 2-oxo-3-pentynoate (6) (16) and 3-bromopropiolate (8) (17). CaaD and *cis*-CaaD were purified as previously described (6, 9) and assayed by following the absorbance decrease at 224 nm for 2 ($\epsilon = 4900 \text{ M}^{-1} \text{ cm}^{-1}$) and 3 ($\epsilon = 2900 \text{ M}^{-1} \text{ cm}^{-1}$), as described previously (6, 9). The Amicon concentrator and the YM3 and YM10 ultrafiltration membranes were obtained from Millipore Corp. (Billerica, MA). Sequencing-grade endoproteinase Glu-C (protease V-8) was purchased from F. Hoffmann-La Roche, Ltd. (Basel, Switzerland). Prepacked PD-10 Sephadex G-25 columns were obtained from Biosciences AB (Uppsala, Sweden). Oligonucleotides for DNA amplification and sequencing were synthesized by Genosys (The Woodlands, TX).

Bacterial Strains, Plasmids, and Growth Conditions. *C. glutamicum* ATCC 13032, the genomic DNA source for the *cg10062* gene,³ was purchased from the American type Culture Collection (Manassas, VA). *Escherichia coli* strain BL21-Gold(DE3) (Stratagene, La Jolla, CA) was used in combination with the T7 expression system (pET3b vector) for expression of wild-type Cg10062 and the four mutants (P1A, R70A, R73A, and E114Q). *C. glutamicum* cells were grown at 37 °C in nutrient broth medium. *E. coli* cells were grown at either 30 °C (for protein expression) or 37 °C (for plasmid preparation) in LB medium supplemented with ampicillin (Ap, 100 $\mu\text{g}/\text{mL}$), as indicated.

General Methods. General procedures for cloning and DNA manipulation were performed as described previously (18). The PCR was carried out in a Perkin-Elmer model 480 DNA thermocycler obtained from Perkin-Elmer Inc. (Wellesley, MA). DNA sequencing was performed by the DNA Core Facility of the Institute for Cellular and Molecular Biology at The University of Texas. The procedures for protein analysis using sodium dodecyl sulfate–polyacrylamide gel electrophoresis (SDS–PAGE) on 15% gels (19) and protein quantification are reported elsewhere (20). The native molecular mass of wild-type Cg10062 was determined by gel filtration on the Superose 12 column. Kinetic data were obtained on a Hewlett-Packard 8452A diode array spectrophotometer or an Agilent 8453 UV–visible spectrophotometer. The kinetic data were fitted by nonlinear regression data analysis using Grafit (Erithacus Software Ltd., Horley, U.K.) obtained from Sigma Chemical Co. Nuclear magnetic resonance (NMR) spectra were recorded in 100% H_2O on a Varian Unity INOVA-500 spectrometer as reported previously (6).

Construction of the Cg10062 Expression Vector. To remove an internal *Bam*HI restriction site, the *cg10062* gene was generated by overlap extension PCR (21). The forward primer (5'-ATACATATGCCTACTTATACT-TGT-3') is designated primer F1 and contains an *Nde*I restriction site (in bold) followed by 15 bases corresponding to the coding sequence of the *cg10062* gene. The reverse primer (5'-CATGGATCCCTATTCTGACGATCC-3') is designated primer R1 and contains a *Bam*HI restriction site (in bold) followed by 15 bases corresponding to the complementary sequence of the *cg10062* gene. The internal PCR primers were oligonucleotides 5'-

³ The Cg10062 protein and gene identification numbers are NP_599314.1 and 19551312, respectively.

CTGATTCTTGAATCCCCAAT-3' and 5'-ATTGGG-GATTCCAAGAATCAG-3', where the silent mutation resulting in deletion of the internal *Bam*HI site is indicated in bold. Total genomic DNA from *C. glutamicum* ATCC 13032 was isolated by a phenol extraction procedure described previously (22). Amplification mixtures contained the appropriate synthetic primers, deoxynucleotide triphosphates, genomic DNA, and PCR reagents supplied in the Expand High Fidelity PCR system. The resulting PCR product and the pET3b vector were digested with *Nde*I and *Bam*HI restriction enzymes, purified, and ligated using T4 DNA ligase. An aliquot of the ligation mixture was transformed into competent *E. coli* BL21-Gold(DE3) cells. Transformants were selected at 37 °C on LB/Ap plates. Plasmid DNA was isolated from several randomly selected colonies and analyzed by restriction analysis for the presence of the insert. The cloned *cg10062* gene was sequenced to verify that no other mutations had been introduced during the amplification of the gene. The newly constructed expression vector was named pET(cg10062).

Construction of the Cg10062 Mutants and Expression and Purification of Wild-Type and Mutant Proteins. The experimental procedures used for the construction of the P1A, R70A, R73A, and E114Q Cg10062 mutants are provided in the Supporting Information. In addition, protocols used for the production and purification of wild-type Cg10062 and the four mutant proteins are reported in the Supporting Information. Finally, the mass spectral analysis of the four mutant proteins can be found in the Supporting Information.

Mass Spectrometric Characterization of Cg10062 and Cg10062 Inactivated by 8. The masses of Cg10062 and Cg10062 inactivated by **8** were determined using an LCQ electrospray ion trap mass spectrometer (Thermo, San Jose, CA), housed in the Analytical Instrumentation Facility Core in the College of Pharmacy at The University of Texas. The protein samples were prepared as described previously (6). The observed monomer mass for Cg10062 was 17092 Da (calcd 17096 Da). The mass for the modified Cg10062 sample is reported below.

¹H NMR Spectroscopic Product Analysis of the Reaction of Cg10062 with 2-Oxo-3-pentynoate (6). The product of the Cg10062-catalyzed hydration of 2-oxo-3-pentynoate (**6**) was identified as acetopyruvate (**7**) by ¹H NMR spectroscopy using a procedure described elsewhere with the following modifications (6, 9). Six individual reaction mixtures consisted of H₂O (800 μL) and an aliquot of **6** (100 μL) from a stock solution. The stock solution of **6** (4 mg, 36 mmol) was created in 100 mM Na₂HPO₄ buffer (pH 9.2, 0.6 mL), and the pH of the solution was adjusted to 7.6 with aliquots of an aqueous 1 M NaOH solution. The stock solution was used immediately after preparation. A quantity of Cg10062 (100 μL of a 3.2 mg/mL solution) was added to each reaction mixture. After 18 h at 4 °C, the reaction mixtures were combined and the enzyme was removed as described previously (6, 9). The effluent was concentrated to ~0.6 mL in vacuo and placed in a NMR tube along with DMSO-*d*₆ (30 μL). The ¹H NMR spectrum shows the presence of signals corresponding to **6**, **7**, the hydrate of **7**, and the enol isomer of **7** (23). Under these conditions, inactivation of Cg10062 was not observed.

¹H NMR Spectroscopic Detection of 4 in the Cg10062-Catalyzed Dehalogenation of 3. A series of ¹H NMR spectra monitoring the Cg10062-catalyzed transformation of *cis*-3-chloroacrylate (**3**) was recorded as follows. An amount of **3** (4 mg, 0.04 mmol) dissolved in DMSO-*d*₆ (30 μL) was added to 100 mM Na₂HPO₄ buffer (0.6 mL, pH ~9) and placed in a NMR tube. The pH of the reaction mixture containing **3** was adjusted to 9.0 using small aliquots of an aqueous 1 M NaOH solution. Subsequently, an aliquot of Cg10062 (50 μL of a 3.2 mg/mL solution of Cg10062) from a solution created in 20 mM Na₂HPO₄ buffer (pH 7.3) was added to the reaction mixture. The first ¹H NMR spectrum was recorded 5 min after the addition of enzyme and every 3 min thereafter for a total reaction time of 32 min. The final pH of the reaction mixture was 7.3. The ¹H NMR spectra showed signals for *cis*-3-chloroacrylate (**3**), malonate semialdehyde (**4**), its hydrate, acetaldehyde (**5**), and its hydrate (**6**). Acetaldehyde presumably results from the nonenzymatic decarboxylation of **4** but could also be due to a promiscuous MSAD activity of Cg10062. The mixture contained ~67% **3**, as assessed by integration of the signals.

¹H NMR Spectroscopic Analysis of Incubation Mixtures Containing 2 and Cg10062 or cis-CaaD. In separate experiments, Cg10062 or *cis*-CaaD was incubated with the *trans* isomer of 3-chloroacrylate (i.e., **2**), and the reactions were followed by ¹H NMR spectroscopy (6). An amount of **2** (4 mg, ~0.04 mmol) dissolved in DMSO-*d*₆ (30 μL) was added to 100 mM Na₂HPO₄ buffer (0.6 mL, pH ~9) and placed in a NMR tube. The pH of the reaction mixtures was adjusted to 9.5. Subsequently, Cg10062 [100 μL of a 22 mg/mL solution in 20 mM Na₂HPO₄ buffer (pH 8.0)] or *cis*-CaaD [40 μL of a 31.1 mg/mL solution in 20 mM Na₂HPO₄ buffer (pH 8.0)] was added to the reaction mixture. Both reaction mixtures were examined by ¹H NMR spectroscopy after an initial incubation period (46 h for Cg10062 and 41 h for *cis*-CaaD) and a lengthy incubation period (6 weeks). To minimize photoisomerization, the NMR tubes containing the reaction mixtures were stored in the dark except when they were analyzed by NMR spectroscopy. After 6 weeks, the mixture of Cg10062 and **2** exhibited signals corresponding to **2** (~6%), **4** (~6%), the hydrate of **4** (~16%), **5** (~30%), and the hydrate of **5** (~41%) (6). The approximate quantities were determined by integration. The ¹H NMR spectra for the mixture containing *cis*-CaaD and **2** exhibited only signals corresponding to **2**.

Kinetic Assays. All the kinetic assays were performed at 23 °C and pH ~9.0. Previous work has shown that the highest *cis*-CaaD activity is observed at this pH (9, 10). The assays used for the colorimetric determination of the dehalogenation of **2** and **3** and to follow the hydration of **6** are based on protocols reported elsewhere (5, 6). The modifications to these assays are provided in the Supporting Information. In a coupled assay, the dehalogenation of **2** by CaaD, **3** by *cis*-CaaD, and **2** or **3** by Cg10062 was monitored by following the production of NADH from NAD⁺ at 340 nm ($\epsilon = 6220 \text{ M}^{-1} \text{ cm}^{-1}$). The assay mixtures (total volume of 1 mL) were created in 20 mM Na₂HPO₄ buffer (pH 9.0) and contained dithiothreitol (0.1 mM), NAD⁺ [350 μM, 10 μL of a 26.5 mg/mL stock solution in 100 mM Na₂HPO₄ buffer (pH 9.0)], aldehyde

dehydrogenase [0.44 mg, 10 μ L of a 44 mg/mL stock solution in 100 mM Na₂HPO₄ buffer (pH 9.0)], FG41 MSAD⁴ [\sim 0.1 mg, 10 μ L of a 9.3 mg/mL stock solution in 10 mM Na₂HPO₄ buffer (pH 8.0)], **2** or **3** [10–150 mM from a 1 M stock solution made up in 100 mM Na₂HPO₄ buffer (pH 9.0)], and CaaD (30 nM), *cis*-CaaD (39 nM), or Cg10062 (0.27 μ M using **2** and 0.07 μ M using **3**). The assays were initiated by the addition of **2** or **3** and followed for 5 min.

¹H NMR Spectroscopic Assay for CaaD and *cis*-CaaD Activities of the P1A, R70A, R73A, and E114Q Cg10062 Mutants. An amount of **2** or **3** (4 mg, \sim 0.04 mmol) dissolved in DMSO-*d*₆ (30 μ L) was added to 100 mM Na₂HPO₄ buffer (0.6 mL, pH \sim 9) and placed in a NMR tube (**6**). The pH of the reaction mixture was adjusted to 9.5. Subsequently, enzyme [\sim 1.0 mg made up in 20 mM Na₂HPO₄ buffer (pH 8.0)] was added to the reaction mixture. The eight reaction mixtures were examined by ¹H NMR spectroscopy after a 17–18 h incubation period, and the product amounts were estimated by integration of the signals corresponding to **2** (or **3**), **4**, **5**, and the corresponding hydrates (**6**), if present. The ¹H NMR signals for these species are reported elsewhere (**6**). The pH after the incubation period ranged between 8.1 and 8.5 for all samples except for the sample containing E114Q and **3**, which had a final pH of 7.3.

Irreversible Inactivation of Cg10062 by **8**, Mass Spectral Analysis, and Peptide Mapping. The enzyme (20 μ M based on the molecular mass of the native enzyme) was incubated with a large excess of **8** (0.5 mM) in 0.5 mL of 20 mM NaH₂PO₄ buffer (pH 7.3) for 28 h at 4 °C (**6**). In a separate control experiment, the same quantity of enzyme was incubated without inhibitor under otherwise identical conditions. Subsequently, the two samples were loaded onto individual PD-10 Sephadex G-25 gel filtration columns, which had previously been equilibrated with 100 mM (NH₄)HCO₃ buffer (pH 8.0). The protein was eluted with the same buffer by gravity flow. Fractions (0.5 mL) were analyzed for the presence of protein by UV absorbance at 214 nm. The purified enzymes were assayed for residual *cis*-CaaD activity using the colorimetric assay for dehalogenation (**5**). The sample treated with **8** had no activity, while the control sample retained full activity. Subsequently, the samples were analyzed by electrospray ionization mass spectrometry (ESI-MS) and used in the following peptide mapping experiments.

For the peptide mapping experiments, a quantity (\sim 25 μ g) of unmodified Cg10062 and Cg10062 inactivated by **8** was dried under vacuum (**6**). The individual protein pellets from the two samples were dissolved in 10 μ L of 10 M guanidine HCl and incubated for 2 h at 37 °C. Subsequently, the protein samples were diluted 10-fold with 100 mM (NH₄)HCO₃ buffer (pH 8.0) and incubated for 48 h at 37 °C with protease V-8 (2.5 μ L of a 10 mg/mL stock solution created in water) (**24**, **25**). The protease V-8-treated samples were made up and analyzed on the delayed extraction Voyager-DE PRO matrix-assisted laser desorption ionization time-of-flight

Table 1: Kinetic Parameters for the Cg10062-, *cis*-CaaD-, and CaaD-Catalyzed Conversion of 2-Oxo-3-pentynoate (**6**) to Acetopyruvate (**7**)^a

enzyme	k_{cat} (s ⁻¹)	K_m (μ M)	k_{cat}/K_m (M ⁻¹ s ⁻¹)
Cg10062	0.33 \pm 0.03	6200 \pm 750	0.05 \times 10 ³
<i>cis</i> -CaaD ^b	0.007 \pm 0.001	620 \pm 60	0.01 \times 10 ³
CaaD ^c	0.7 \pm 0.02	110 \pm 4	6.4 \times 10 ³

^a The steady-state kinetic parameters were determined in 20 mM Na₂HPO₄ buffer (pH 9.0) at 23 °C. Errors are standard deviations.

^b These parameters were obtained from ref 9. ^c These parameters were obtained from ref 6.

(MALDI-TOF) instrument (PerSeptive Biosystems, Framingham, MA) as previously described (**6**). Selected ions of the samples were also subjected to MALDI-PSD analysis using the protocol described previously to identify the covalently modified residue (**26**).

RESULTS

Expression, Purification, and Characterization of Cg10062. The *cg10062* gene was amplified from genomic DNA of *C. glutamicum* and fused into the start codon of expression vector pET3b, resulting in the pET(*cg10062*) construct. The *cg10062* gene in pET(*cg10062*) is under the control of a T7 promoter, and the enzyme was produced constitutively in a soluble and active form in *E. coli* BL21(DE3). The recombinant enzyme was purified by two methods. For all experiments except those involving low-level activities, the cell lysate was routinely processed through two HPLC columns (anion exchange and hydrophobic interaction), followed by a gel filtration step (if necessary). For the identification and quantification of low-level activities, the cell lysate was processed similarly but passed through hand-packed disposable columns. Typically, both procedures yield \sim 50 mg of homogeneous protein per liter of culture. The subunit and native molecular masses were determined to be 17092 \pm 2 Da and \sim 50 kDa, respectively. A comparison of these values to the calculated subunit mass (17227 Da) indicates that the initiating methionine is removed during posttranslational processing, resulting in a protein with an N-terminal proline, and suggests that the native enzyme is a homotrimeric protein.

Hydration of 2-Oxo-3-pentynoate (6) by Cg10062. It has previously been determined that CaaD and *cis*-CaaD function as hydratases and convert 2-oxo-3-pentynoate (**6**, Scheme 2) to acetopyruvate (**7**) (**6**, **9**). These observations prompted us to examine whether Cg10062 catalyzes the hydration of **6**. The results show that Cg10062 converts **6** to **7** and that the catalytic efficiency is slightly higher than that observed for *cis*-CaaD (**9**). The identity of **7** was confirmed by ¹H NMR spectroscopy. The ¹H NMR spectrum exhibited signals consistent with the structure of **7**, as well as two additional species, the hydrate of **7** and the enol of **7** (**6**). We have previously shown that **6** is stable for several hours in solution and does not decompose to **7** (**6**). Cg10062 is inactivated by high concentrations of **6** ($>$ 60 mM) with no detectable conversion of **6** to **7**.

The kinetic parameters for the conversion of **6** to **7** by Cg10062 and those previously measured for *cis*-CaaD and CaaD are summarized in Table 1. A comparison of these parameters indicates that the k_{cat} value for Cg10062 is 47-fold higher than that measured for *cis*-CaaD while the K_m

⁴ FG41 MSAD is a MSAD homologue found in coryneform bacterium strain FG41. Although FG41 MSAD and MSAD from *P. pavonaceae* 170 are only 37% identical in sequence, they have comparable decarboxylase activities, but the FG41 MSAD lacks a hydratase activity (H. Serrano, G. J. Poelarends, W. H. Johnson, Jr., and C. P. Whitman, 2008, unpublished results).

Table 2: Kinetic Parameters for CaaD- and *cis*-CaaD-Catalyzed Dehalogenation of **2** and **3**

enzyme	substrate	assay	K_m (μM)	k_{cat} (s^{-1})	k_{cat}/K_m ($\text{M}^{-1} \text{s}^{-1}$)
CaaD	2	224 nm ^a	49 ± 5	1.9 ± 0.1	3.9 × 10 ⁴
CaaD	2	coupled ^b	28 ± 3	1.9 ± 0.6	6.8 × 10 ⁴
CaaD	2	colorimetric ^c	ND ^d	1.5	ND ^d
<i>cis</i> -CaaD	3	224 nm ^a	34 ± 8	1.8 ± 0.2	5.3 × 10 ⁴
<i>cis</i> -CaaD	3	coupled ^b	152 ± 20	4.6 ± 0.3	3.0 × 10 ⁴
<i>cis</i> -CaaD	3	colorimetric ^c	ND ^d	1.0	ND ^d

^a The kinetic parameters were measured in 20 mM Na₂HPO₄ buffer (pH 9.0) at 22 °C following the decrease in absorbance at 224 nm. Errors are standard deviations. ^b The kinetic parameters were measured in 20 mM Na₂HPO₄ buffer (pH 9.0) at 22 °C. Errors are standard deviations. ^c The kinetic parameters were measured in 50 mM Tris-SO₄ buffer (pH 9.0) at 22 °C. Errors are standard deviations. ^d Not determined.

value is 10-fold higher. The net effect is a 5-fold higher k_{cat}/K_m value. In contrast, the k_{cat} value for CaaD is ~2-fold higher than that measured for Cg10062 while the K_m value is ~56-fold lower. As a result, the k_{cat}/K_m value for CaaD is ~130-fold higher than that observed for Cg10062.

Dehalogenation of 2 and 3 by Cg10062. The level of sequence identity with *cis*-CaaD and the hydratase activity suggested that Cg10062 might function as a *cis*-CaaD. However, the low *cis*-CaaD activity (and CaaD activity) of Cg10062 precluded the use of a previously described assay, which follows the decrease in substrate absorbance at 224 nm (9). The absorbance of the large amount of substrate and protein required to produce a detectable reaction rate does not permit accurate measurements at 224 nm. Hence, a coupled assay was developed that follows the formation of NADH from NAD⁺. In this assay, dehalogenation of **2** or **3** produces **4**, which is decarboxylated by MSAD to afford acetaldehyde (**5**). The large excess of aldehyde dehydrogenase converts **5** to acetate, and the oxidation of **5** is coupled to the reduction of NAD⁺. The kinetic parameters for CaaD and *cis*-CaaD with their respective isomers were determined by this coupled assay and compared with those measured by the 224 nm assay and a previously described colorimetric assay (5) (Table 2). For CaaD, the kinetic parameters are comparable (<2-fold difference). For *cis*-CaaD, the K_m and k_{cat} values determined using the coupled assay are higher (~4.5- and ~2.5-fold, respectively), but the overall k_{cat}/K_m values are comparable. The higher values may be a more accurate reflection of the *cis*-CaaD activity because the absorbance at 224 nm is not the λ_{max} for **3** but rather corresponds to a shoulder. The colorimetric assay, which monitors halide release, is not accurate at substrate concentrations of <400 μM , so K_m values cannot be measured (5).

Using the coupled assay and the colorimetric assay, the dehalogenase activity for Cg10062 with **2** and **3** was determined (Table 3). A comparison of the parameters measured in the coupled assay shows that the K_m values are significantly higher than those measured for CaaD and *cis*-CaaD (~2800- and ~125-fold, respectively). The k_{cat} value for Cg10062 using the *trans* isomer is ~32-fold lower than that determined for CaaD. The k_{cat} value for Cg10062 using the *cis* isomer is comparable to that of *cis*-CaaD. Overall, the k_{cat}/K_m values show that Cg10062 is much less efficient in processing the *trans* isomer than CaaD is (~8.5 × 10⁴-fold). Cg10062 clearly prefers the *cis* isomer, but does not process it as efficiently as *cis*-CaaD (~160-fold). The values

Table 3: Kinetic Parameters for the Cg10062-Catalyzed Dehalogenation of **2** and **3**

enzyme	substrate	assay	K_m (mM)	k_{cat} (s^{-1})	k_{cat}/K_m ($\text{M}^{-1} \text{s}^{-1}$)
Cg10062	2	coupled ^a	78 ± 36	0.06 ± 0.01	0.8
Cg10062	2	colorimetric ^b	54 ± 40	0.002 ± 0.001	0.04
Cg10062	3	coupled ^a	19 ± 1	3.5 ± 1.1	184
Cg10062	3	colorimetric ^b	156 ± 42	1.6 ± 0.3	10

^a The kinetic parameters were measured in 20 mM Na₂HPO₄ buffer (pH 9.0) at 22 °C. Errors are standard deviations. ^b The kinetic parameters were measured in 50 mM Tris-SO₄ buffer (pH 9.0) at 22 °C. Errors are standard deviations.

measured in the colorimetric assay are in accord with these observations. However, in contrast to CaaD and *cis*-CaaD, Cg10062 processes both isomers.

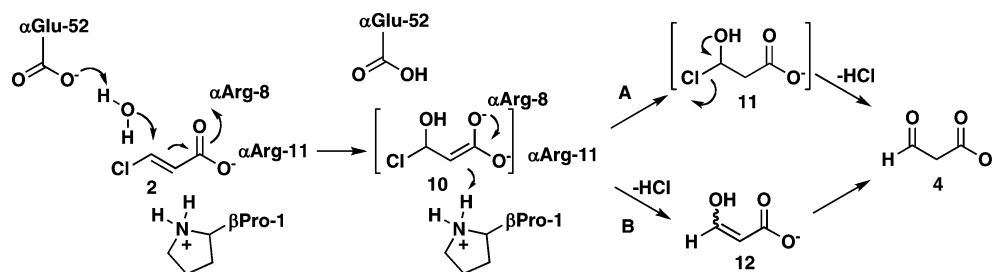
Mixtures containing Cg10062 and either the *cis* or *trans* isomer were monitored by ¹H NMR spectroscopy to verify that the product of these reactions is **4**, which was previously established for the *cis*-CaaD- and CaaD-catalyzed reactions (6, 9). Indeed, the enzymatic conversion of **2** or **3** yields **4**, as indicated by a doublet at 3.20 ppm and a triplet at 9.50 ppm (data not shown), which correspond to the protons at C-2 and C-3, respectively (6). In addition, signals corresponding to the hydrate of **4** are present. Hence, **4** is the product of the Cg10062-catalyzed conversion of **2** and **3**. For the reaction of Cg10062 and **3**, the reaction was ~33% complete after 32 min.

By NMR spectroscopy, it took a significant period of time (~6 weeks) to detect product using Cg10062 and the *trans* isomer (i.e., **2**). The lengthy incubation period prompted us to examine (by NMR spectroscopy) whether *cis*-CaaD processed the *trans* isomer after a comparable incubation period. After 6 weeks, there was no detectable product formation in the incubation mixture containing *cis*-CaaD and **2**, whereas the mixture containing Cg10062 and **2** was ~95% complete.

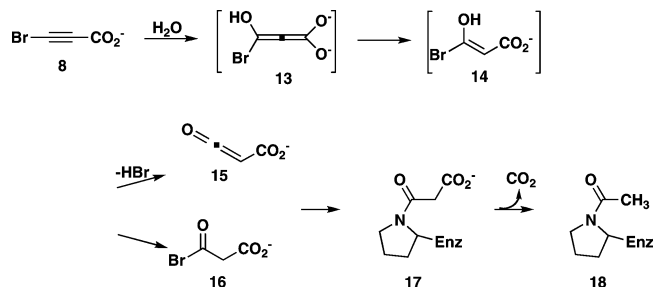
Construction and Kinetic and ¹H NMR Analysis of the P1A, R70A, R73A, and E114Q Cg10062 Mutants. Four residues present in Cg10062 (Pro-1, Arg-70, Arg-73, and Glu-114) have counterparts in *cis*-CaaD and CaaD that have been identified as critical active site residues. Hence, four site-directed mutants were constructed (P1A, R70A, R73A, and E114Q Cg10062) and purified so the importance of these residues to the dehalogenation of **2** and **3** could be examined. The mutants have no detectable dehalogenase activity using the colorimetric assay (after an overnight incubation) and no detectable hydratase activity (using **6**). These results are not surprising in view of the low activities of the wild-type enzyme. Nonetheless, the results suggest that all four residues are required for the dehalogenation of **2** and **3** and the hydration of **6**.

The dehalogenase activities of the four mutants were also assessed by ¹H NMR spectroscopy after a 17–18 h incubation period. Using the *cis* isomer (**3**), the E114Q-catalyzed reaction was 100% complete and the P1A-catalyzed reaction showed a trace amount of product (**4** and the hydrate), but not a sufficient amount for quantification. Mixtures containing the R70A and R73A Cg10062 mutants showed no product. The observations parallel those observed for *cis*-CaaD using **3** and suggest that Pro-1, Arg-70, and Arg-73 are more critical for the *cis*-CaaD activity of Cg10062 than Glu-114. Using the *trans* isomer (**2**), the E114Q-catalyzed reaction results in 4% product. Mixtures containing the P1A,

Scheme 3



Scheme 4



R70A, and R73A Cg10062 mutants showed no product. Again, Pro-1, Arg-70, and Arg-73 are more critical for the CaaD activity of Cg10062 than Glu-114.

Irreversible Inhibition of Cg10062 by 8. It is well established that 3-bromopropionate (**8**, Scheme 2) irreversibly inhibits CaaD and *cis*-CaaD (6, 9). The inhibition results from the covalent modification of the catalytic Pro-1 by a species formed as a result of the enzyme-catalyzed hydration of **8** (Scheme 4) (6, 8, 9). In view of the hydratase activity of Cg10062, we anticipated that **8** would also lead to irreversible inhibition of Cg10062. After a 28 h incubation period (at 4 °C) with **8**, Cg10062 was irreversibly inhibited. Gel filtration chromatography did not result in recovery of enzyme activity, indicating that a covalent bond has formed between Cg10062 and a species (either **15** or **16** in Scheme 4) derived from the enzymatic hydration of **8**.

ESI-MS Analysis of the Inactivated Cg10062. To identify the species resulting in the covalent modification of Cg10062, the enzyme was incubated with **8**, and the inactivated protein was isolated and analyzed by ESI-MS. A control sample containing only Cg10062 was processed and analyzed similarly. Mass spectral analysis of the Cg10062 control sample showed one major peak corresponding to a mass of 17092 ± 2 Da. Mass spectral analysis of Cg10062 incubated with **8** showed two major peaks corresponding to masses of 17134 ± 2 and 17178 ± 2 Da. The mass of the latter species (i.e., 17178 Da) is in agreement with that expected for the enzyme modified with a 3-oxopropionate group (+86 Da), the adduct resulting from the enzyme-catalyzed hydration of **8** (**17** in Scheme 4). This observation is consistent with the mass spectral analysis of CaaD and *cis*-CaaD inactivated by **8**, which are also modified by a molecule with a mass of 86 Da (6, 8, 9). The species with a mass of 17134 Da, however, reveals the addition of a covalent adduct having a mass of 42 Da. This adduct (**18** in Scheme 4) most likely represents the same label, but in this case, the 3-oxopropionate moiety, a β -keto acid, has lost CO_2 .⁵

Identification of the Modified Residue by Mass Spectrometry. The site of the modification was first localized to a peptide fragment of Cg10062 by digesting the modified and

Table 4: PSD Fragment Ions of the Peptide Fragment from Pro-1 to Glu-15 from Cg10062 and Cg10062 Treated with **8**

sample	observed or calculated PSD fragment ion mass ^a		
	P-immonium ion	b ₁	b ₂
calculated	70.1	98.1	199.2
Cg10062 peptide	70.1	ND ^b	199.0
covalently modified peptide	111.9	139.7	240.8

^a The immonium ion has lost the CO group of the peptide amide, while the b ion retains this group. ^b Not detected.

unmodified Cg10062 samples with protease V-8 and analyzing the resulting peptide mixtures by MALDI-MS. Under the incubation mixture conditions, protease V-8 cleaves peptide bonds preferentially at the carboxylate side of glutamate residues (24, 25). There are 23 glutamate residues in Cg10062 so that a complete digestion will result in 24 fragments or amino acid residues. This analysis assumes that there is no hydrolytic cleavage of the peptide bond at the carboxylate side of the two aspartate residues. A comparison of the peaks for the modified and unmodified Cg10062 samples revealed a single modification by a species having a mass of 42 Da on the peptide fragment from Pro-1 to Glu-15.⁵ Analysis of the remaining peaks showed no modification of other fragments (data not shown).

To determine the single covalently modified residue, selected peaks observed in the protease V-8-digested control sample and in the protease V-8-digested sample treated with **8** were subjected to MALDI-PSD fragmentation analysis (Table 4) (26). The PSD spectrum of the ion corresponding to the unlabeled peptide (Pro-1 to Glu-15) displays the characteristic immonium ion at m/z 70.1 (resulting from Pro-1) and N-terminal sequence-specific fragment ion b₂, which results from the dipeptide, Pro-1-Thr-2 [Cg10062 peptide (Table 4)]. MALDI-PSD fragmentation analysis of the ion corresponding to the peptide modified by a species derived from **8** shows an increase in mass of 42 Da for the b₂ fragment ion [covalently modified Cg10062 peptide (Table 4)]. Thus, only Pro-1 and Thr-2 remain as potential targets of alkylation. Further evidence implicating Pro-1 as the site of modification was provided by the presence of the immonium and b₁ fragment ions in the PSD spectrum of the modified peptide, with mass values consistent with the covalent attachment of a single species with a mass of 42 Da to the Pro-1 residue (Table 4). While the b₁ ion,

⁵ ESI-MS analysis of Cg10062 treated with **8** shows two species with molecular masses of 42 and 86 Da. However, the MALDI-MS spectrum shows only one species with a molecular mass of 42 Da. We have previously attributed this observation to the matrix-induced loss of the CO_2 group from the 3-oxopropionate adduct, a β -keto acid (6, 8, 9).

corresponding to the fragmentation of Pro-1, is not normally observed in PSD spectra (26), it is apparently stabilized by its modification with the adduct, accounting for the presence of this ion in the spectrum of the sample treated with **8**.

DISCUSSION

Sequence analysis, crystallographic observations, and the results of mechanistic, mutagenesis, and inhibition studies have established working hypotheses for the CaaD and *cis*-CaaD mechanisms (Scheme 3) (5–11). For CaaD, α Glu-52 activates a water molecule for attack at C-3 and α Arg-8 and α Arg-11 bind and interact with the C-1 carboxylate group (8). This interaction likely draws electron density away from C-3, thereby creating a partial positive charge and enhancing the electrophilicity of C-3. The proposed enediolate intermediate, **10**, can rearrange with protonation at C-2 (from β Pro-1) to generate the unstable halohydrin species **11** (Scheme 3A). Subsequent chemical or enzymatic decay produces **4**. Alternatively, the enediolate can rearrange to eliminate the halide and form an enol intermediate (**12**, Scheme 3B). Subsequent formation of the carbonyl group and protonation at C-2 (by β Pro-1) afford **4**. Recent work implicates the enol intermediate in Scheme 3B, but the scenario shown in Scheme 3A cannot be ruled out (27). The proposed mechanism for *cis*-CaaD is largely the same except two additional residues, His-28 and Tyr-103, are involved (11). It is proposed that His-28 assists Arg-70 and Arg-73 in the binding and activation of substrate and Tyr-103 assists Glu-114 in the activation of the water molecule for attack at C-3. Pro-1 again provides the proton at C-2.

A comparison of the structure of CaaD inactivated by **8** with those of *cis*-CaaD (both native and one inactivated by an epoxide) suggests that the different active site shapes and substrate orientations might govern isomer specificity (11). The active site of CaaD is elongated, and the interaction of the substrate's carboxylate group with the two arginine residues projects the substrate into the enzyme. In contrast, the active site of *cis*-CaaD is more U-shaped, and His-28 (along with Arg-70 and Arg-73) directs the substrate toward the surface of the enzyme. Modeling studies show that the 3-chloro group of the *cis* isomer could bind in a pocket formed by Thr-34, Leu-38, Leu-119, and Arg-70 (11). These same studies indicate that Tyr-103 would effectively block the binding of the 3-chloro group of a *trans* substrate.

The high degree of sequence similarity between Cg10062 and *cis*-CaaD (~53%) coupled with the conservation of the six key active site residues suggested that Cg10062 would behave like *cis*-CaaD and function as an isomer-specific dehalogenase. Studies with 2-oxo-3-pentynoate (**6**, Scheme 2) support this view. Cg10062 catalyzes the hydration of **6** to produce acetopyruvate (**7**) with a catalytic efficiency somewhat better than that observed for the *cis*-CaaD reaction (as assessed by k_{cat}/K_m values) (9). However, both reactions are significantly less efficient than CaaD, which is rationalized by the fact that the elongated active site of CaaD can more easily accommodate the linear acetylene molecule (5, 9). The observation that Cg10062 processes **6** instead of being inactivated by **6** implies that Pro-1 has a pK_a comparable to that determined for CaaD and *cis*-CaaD (~9.2) (7, 10). A growing body of evidence suggests that the reaction of **6** with tautomerase superfamily members reflects the predomi-

nant ionization state of Pro-1 (neutral vs cationic) (28, 29). For example, the incubation of CaaD, *cis*-CaaD, and MSAD with **6** results in the conversion of **6** to **7** due to the cationic Pro-1 and these enzymes' ability to carry out a hydration reaction (5, 9, 28, 29). In contrast, 4-oxalocrotonate tautomerase (4-OT) and a 4-OT homologue from *Bacillus subtilis* designated YwhB are irreversibly inactivated by **6** because Pro-1 is neutral in these enzymes (at physiological pH), allowing them to function as bases with pK_a values of ~6.4⁶ (16, 30).

The results of the studies with **8** also show that Cg10062 and *cis*-CaaD function similarly. The 3-halopropiolates (i.e., **8** and **9**, Scheme 2) have been shown previously to be irreversible inhibitors of CaaD, *cis*-CaaD, and MSAD (5, 9, 12). In all three cases, Pro-1 is modified by a 3-oxopropanoate moiety (**17** in Scheme 4), and two possible mechanisms for generating this adduct have been proposed (5, 8, 9, 12, 13). For CaaD, *cis*-CaaD, and MSAD, inactivation proceeds through the enzyme-mediated attack of water at C-3 of **8** (Scheme 4). The resulting allenic species **13** rearranges to **14**, which can then decompose by two routes. In one route, direct expulsion of the bromide produces a ketene (i.e., **15**) which can modify Pro-1. In a second route, tautomerization of **14** (and protonation at C-2) yields acyl bromide **16**. Subsequent acylation of Pro-1 by **16** inactivates the enzyme. It is postulated that Pro-1 becomes nucleophilic as a consequence of the initial hydration of **8** by the enzyme.

Clearly, Cg10062 functions as a hydratase using **6** and **8**, and its behavior with these compounds largely mirrors that of *cis*-CaaD. However, in spite of these similarities, Cg10062 is a poor *cis*-CaaD: it has a much lower catalytic efficiency, and it does not display absolute specificity for the *cis* isomer. The lower catalytic efficiency stems from the much higher K_m value, which suggests suboptimal binding of the *cis* isomer in the active site of Cg10062. Unlike that of *cis*-CaaD, the active site of Cg10062 can also accommodate and process the *trans* isomer, albeit poorly. The lower catalytic efficiency of this reaction (in comparison to the k_{cat}/K_m of the CaaD-catalyzed reaction) results from a higher K_m value combined with a lower k_{cat} . The lower affinity for the substrate could again be due to suboptimal alignment, whereas the lower k_{cat} value could be due to an effect on the reaction chemistry, product release, or both. The mutagenesis results (for Pro-1, Arg-70, Arg-73, and Glu-114) invoke roles for these residues in the dehalogenase activities of Cg10062. These observations indicate that dehalogenation is active site-dependent and not the consequence of a nonspecific encounter between Cg10062 and substrate.

Although Cg10062 is not an efficient *cis*-CaaD or CaaD, the rates of dehalogenation are still impressive in comparison with the reported nonenzymatic rate (31). Horvat and Wolfenden reported that the uncatalyzed rate is $\sim 2.2 \times 10^{-12} \text{ s}^{-1}$ at 25 °C (31). Hence, Cg10062 shows an $\sim 1.6 \times 10^{12}$ -fold rate enhancement using the *cis* isomer and a 9.0×10^8 - to 2.7×10^{10} -fold rate enhancement using the *trans* isomer. By comparison, *cis*-CaaD exhibits a 2.1×10^{12} -fold rate enhancement.

⁶ Like *cis*-CaaD, inactivation of Cg10062 is observed at higher concentrations of **6** (>60 mM) (6, 8). This may be a function of the enzyme's slow processing of **6** coupled with presence of both neutral and cationic Pro-1 at pH 9.2.

It was initially thought that the much higher K_m values (assuming K_m reflects substrate binding) result from a more spacious Cg10062 active site where larger side chain groups found in *cis*-CaaD are replaced with smaller side chains in Cg10062. As a result, the active site of Cg10062 could accommodate both isomers, but they would bind with much lower affinity. An examination of the *cis*-CaaD crystal structure shows that the active site pocket is defined by Pro-1, His-28, Thr-32, Thr-34, His-69, Arg-70, Arg-73, Tyr-103, Met-112, and Glu-114 (9). As most of these same residues are found in Cg10062, the active site is unlikely to be more spacious.

There are, however, two intriguing exceptions. First, His-69 in *cis*-CaaD is replaced with an isoleucine in Cg10062. In *cis*-CaaD, His-28 and His-69 interact with the hydroxyl group of Tyr-3. The significance of this interaction is not known, but one possibility is that it positions His-28 for the interaction with the C-1 carboxylate group of the substrate. The presence of the uncharged, hydrophobic isoleucine could alter the position and/or modulate the properties of His-28 or otherwise change the properties of the active site.

The second, more striking exception involves an eight-residue loop that connects the α -helix of a β - α - β motif to the second β -strand. In *cis*-CaaD, Thr-32 and Thr-34 are part of this loop that is made up of Leu-31, Thr-32, Gly-33, Thr-34, Gln-35, His-36, Phe-37, and Leu-38. The same loop in Cg10062 is significantly different, consisting of Leu-31, Ala-32, His-33, Ala-34, Pro-35, Lys-36, Tyr-37, and Leu-38. As noted earlier, Thr-34 may be part of a pocket for the binding of the 3-chloro group of the *cis* substrate. If the binding is mediated by a hydrogen bond from Thr-34, this interaction is no longer possible in Cg10062. Moreover, Gly-33 of *cis*-CaaD is replaced with the bulky, charged His-33, and Gln-35 (in *cis*-CaaD) is replaced with the rigid Pro-35. How these changes affect the properties of the loop and whether this loop plays a role in catalysis and/or specificity are not known. Crystallographic and mutagenesis studies of Cg10062 serve as the starting point for addressing these questions and are being pursued.

Loops can frequently determine specificity, which has been documented well in the enolase superfamily (32, 33). The members of this superfamily are characterized by a (β/α)₈ barrel (the so-called TIM barrel) and a capping domain (32). The capping domain consists of two short loops. The active sites of enolase superfamily members are located at the interfaces of the two domains, where barrel residues function as catalytic groups and loop residues confer specificity to the individual members (33). A similar arrangement could be operative in *cis*-CaaD with some modifications. One possibility is that the catalytic groups are located in the core β - α - β motif and additional determinants of specificity (and perhaps catalysis) come from the loop residues. Moreover, the position of the loop may exclude binding of the *trans* isomer in *cis*-CaaD but allow it in Cg10062.

The sum of these observations suggests that Cg10062 could be a few mutations away from a highly specific and efficient *cis*-CaaD. Although Cg10062 is not necessarily the progenitor for a *cis*-CaaD, it could be representative of one. In one scenario, this progenitor, like Cg10062, has the core

catalytic machinery for a hydration reaction but lacks specificity for the *cis* isomer. Mutations in the loop accompanied by the conversion of Ile-69 to a histidine might provide the additional elements and complete the evolution of Cg10062 to *cis*-CaaD. The consequences of these mutations are currently being examined.

These results do not, however, give any hints about the physiological role of Cg10062 in *C. glutamicum*. This strain was isolated after the introduction of 1,3-dichloropropene (**1**, Scheme 1) into the environment (34). However, BLAST searches of the genome did not identify candidates for other genes in the pathway, indicating that a catabolic pathway for **1** is not likely present.⁷ Nonetheless, the sequence and functional properties suggest that Cg10062 is part of the subfamily of β - α - β fold enzymes from which *cis*-CaaD originated, and it could be representative of a progenitor. This proposed relationship between Cg10062 and *cis*-CaaD and the lack of an obvious genomic context for Cg10062 raise intriguing questions for a future investigation into the biological function of Cg10062 in *C. glutamicum*. Mutational and transcriptional analysis of the *cg10062* gene to define the conditions under which it is expressed would be one step toward understanding the physiological relevance of Cg10062.

ACKNOWLEDGMENT

We thank Steve D. Sorey (Department of Chemistry, The University of Texas) for his assistance in acquiring the NMR spectra. We thank Dr. Gottfried K. Schroeder for insightful discussions.

SUPPORTING INFORMATION AVAILABLE

Experimental procedures for the production and purification of wild-type Cg10062, the construction, production, purification, and mass spectral analysis of the P1A, R70A, R73A, and E114Q Cg10062 mutants, and the assays for the hydratase and dehalogenase activities. This material is available free of charge via the Internet at <http://pubs.acs.org>.

REFERENCES

1. Hartmans, S., Jansen, M. W., van der Werf, M. J., and de Bont, J. A. M. (1991) Bacterial metabolism of 3-chloroacrylic acid. *J. Gen. Microbiol.* 137, 2025–2032.
2. van Hylckama Vlieg, J. E. T., and Janssen, D. B. (1992) Bacterial degradation of 3-chloroacrylic acid and the characterization of *cis*- and *trans*-specific dehalogenases. *Biodegradation* 2, 139–150.
3. Poelarends, G. J., Wilkens, M., Larkin, M. J., van Elsas, J. D., and Janssen, D. B. (1998) Degradation of 1,3-dichloropropene by *Pseudomonas cichorii* 170. *Appl. Environ. Microbiol.* 64, 2931–2936.
4. Poelarends, G. J., and Whitman, C. P. (2004) Evolution of enzymatic activity in the tautomerase superfamily: Mechanistic and structural studies of the 1,3-dichloropropene catabolic enzymes. *Bioorg. Chem.* 32, 376–392.
5. Poelarends, G. J., Saunier, R., and Janssen, D. B. (2001) *trans*-3-Chloroacrylic acid dehalogenase from *Pseudomonas pavonaceae* 170 shares structural and mechanistic similarities with 4-oxalocrotonate tautomerase. *J. Bacteriol.* 183, 4269–4277.
6. Wang, S. C., Person, M. D., Johnson, W. H., Jr., and Whitman, C. P. (2003) Reactions of *trans*-3-chloroacrylic acid dehalogenase with acetylene substrates: Consequences of and evidence for a hydration reaction. *Biochemistry* 42, 8762–8773.
7. Azurmendi, H. F., Wang, S. C., Massiah, M. A., Poelarends, G. J., Whitman, C. P., and Mildvan, A. S. (2004) The roles of active-site residues in the catalytic mechanism of *trans*-3-chloroacrylic acid dehalogenase: A kinetic, NMR, and mutational analysis. *Biochemistry* 43, 4082–4091.

⁷ G. J. Poelarends and C. P. Whitman, 2008, unpublished results.

8. de Jong, R. M., Brugman, W., Poelarends, G. J., Whitman, C. P., and Dijkstra, B. W. (2004) The X-ray structure of *trans*-3-chloroacrylic acid dehalogenase reveals a novel hydration mechanism in the tautomerase superfamily. *J. Biol. Chem.* 279, 11546–11552.
9. Poelarends, G. J., Serrano, H., Person, M. D., Johnson, W. H., Jr., Murzin, A. G., and Whitman, C. P. (2004) Cloning, expression, and characterization of a *cis*-3 chloroacrylic acid dehalogenase: Insights into the mechanistic, structural, and evolutionary relationship between isomer-specific 3-chloroacrylic acid dehalogenases. *Biochemistry* 43, 759–772.
10. Poelarends, G. J., Serrano, H., Johnson, W. H., Jr., and Whitman, C. P. (2004) Stereospecific alkylation of *cis*-chloroacrylic acid dehalogenase by (*R*)-oxirane-2-carboxylate: Analysis and mechanistic implications. *Biochemistry* 43, 7187–7196.
11. de Jong, R. M., Bazzacco, P., Poelarends, G. J., Johnson, W. H., Jr., Kim, Y.-J., Burks, E. A., Serrano, H., Thunnissen, A.-M. W. H., Whitman, C. P., and Dijkstra, B. W. (2007) Crystal structures of native and inactivated *cis*-3-chloroacrylic acid dehalogenase: Structural basis for substrate specificity and inactivation by (*R*)-oxirane-2-carboxylate. *J. Biol. Chem.* 282, 2440–2449.
12. Poelarends, G. J., Johnson, W. H., Jr., Murzin, A. G., and Whitman, C. P. (2003) Mechanistic characterization of a bacterial malonate semialdehyde decarboxylase: Identification of a new activity in the tautomerase superfamily. *J. Biol. Chem.* 278, 48674–48683.
13. Almud, J. J., Poelarends, G. J., Johnson, W. H., Jr., Serrano, H., Hackert, M. L., and Whitman, C. P. (2005) Crystal structures of the wild-type, P1A mutant, and inactivated malonate semialdehyde decarboxylase: A structural basis for the decarboxylase and hydratase activities. *Biochemistry* 44, 14818–14827.
14. Murzin, A. G. (1996) Structural classification of proteins: New superfamilies. *Curr. Opin. Struct. Biol.* 6, 386–394.
15. Whitman, C. P. (2002) The 4-oxalocrotonate tautomerase family of enzymes: How nature makes new enzymes using a β - α - β structural motif. *Arch. Biochem. Biophys.* 402, 1–13.
16. Johnson, W. H., Jr., Czerwinski, R. M., Fitzgerald, M. C., and Whitman, C. P. (1997) Inactivation of 4-oxalocrotonate tautomerase by 2-oxo-3-pentynoate. *Biochemistry* 36, 15724–15732.
17. Andersson, K. (1972) Additions to propiolic and halogen substituted propiolic acids. *Chem. Scr.* 2, 117–120.
18. Sambrook, J., Fritsch, E. F., and Maniatis, T. (1989) *Molecular Cloning: A Laboratory Manual*, Cold Spring Harbor Laboratory Press, Plainview, NY.
19. Laemmli, U. K. (1970) Cleavage of structural proteins during the assembly of the head of bacteriophage T4. *Nature* 227, 680–685.
20. Waddell, W. J. (1956) A simple ultraviolet spectrophotometric method for the determination of protein. *J. Lab. Clin. Med.* 48, 311–314.
21. Ho, S. N., Hunt, H. D., Horton, R. M., Pullen, J. K., and Pease, L. R. (1989) Site-directed mutagenesis by overlap extension using the polymerase chain reaction. *Gene* 77, 51–59.
22. Burks, E. A., Jr., and Whitman, C. P. (1998) Stereochemical and isotopic labeling studies of 2-oxo-hept-4-ene-1,7-dioate hydratase: Evidence for an enzyme-catalyzed ketonization step in the hydration reaction. *J. Am. Chem. Soc.* 120, 7665–7675.
23. Guthrie, J. P. (1972) Acetopyruvic acid. Rate and equilibrium constants for hydration and enolization. *J. Am. Chem. Soc.* 94, 7020–7024.
24. Sorensen, S. B., Sørensen, T. L., and Breddam, K. (1991) Fragmentation of proteins by *S. aureus* strain V8 protease. Ammonium bicarbonate strongly inhibits the enzyme but does not improve the selectivity for glutamic acid. *FEBS Lett.* 294, 195–197.
25. Houmar, J., and Drapeau, G. R. (1972) Staphylococcal protease: A proteolytic enzyme specific for glutamoyl bonds. *Proc. Natl. Acad. Sci. U.S.A.* 69, 3506–3509.
26. Person, M. D., Monks, T. J., and Lau, S. S. (2003) An integrated approach to identifying chemically induced posttranslational modifications using comparative MALDI-MS and targeted HPLC-ESI-MS/MS. *Chem. Res. Toxicol.* 16, 598–608.
27. Poelarends, G. J., Johnson, W. H., Jr., Serrano, H., and Whitman, C. P. (2007) Phenylpyruvate tautomerase activity of *trans*-3-chloroacrylic acid dehalogenase: Evidence for an enol intermediate in the dehalogenase reaction? *Biochemistry* 46, 9596–9604.
28. Poelarends, G. J., Serrano, H., Johnson, W. H., Jr., Hoffman, D. W., and Whitman, C. P. (2004) The hydratase activity of malonate semialdehyde decarboxylase: Mechanistic and evolutionary implications. *J. Am. Chem. Soc.* 126, 15658–15659.
29. Poelarends, G. J., Serrano, H., Johnson, W. H., Jr., and Whitman, C. P. (2005) Inactivation of malonate semialdehyde decarboxylase by 3-halopropiolates: Evidence for hydratase activity. *Biochemistry* 44, 9375–9381.
30. Wang, S. C., Johnson, W. H., Jr., Czerwinski, R. M., and Whitman, C. P. (2004) Reactions of 4-oxalocrotonate tautomerase and YwhB with 3-halopropiolic acids: Analysis and implications. *Biochemistry* 43, 748–758.
31. Horvat, C. M., and Wolfenden, R. V. (2005) A persistent pesticide residue and the unusual catalytic proficiency of a dehalogenating enzyme. *Proc. Natl. Acad. Sci. U.S.A.* 102, 16199–16202.
32. Glasner, M. E., Gerlt, J. A., and Babbitt, P. C. (2006) Evolution of enzyme superfamilies. *Curr. Opin. Chem. Biol.* 10, 492–497.
33. Vick, J. E., and Gerlt, J. A. (2007) Evolutionary potential of (β / α)₈-barrels: Stepwise evolution of a “new” reaction in the enolase superfamily. *Biochemistry* 46, 14589–14597.
34. Ikeda, M., and Nakagawa, S. (2003) The *Corynebacterium glutamicum* genome: Features and impacts on biotechnological processes. *Appl. Microbiol. Biotechnol.* 62, 99–109.

BI8007388